JACS
JOURNAL OF THE AMERICAN CHEMICAL SOCIETY

ARTICLE

pubs.acs.org/JACS

Mechanism of N/O Bond Scission of N_2O by an Unsaturated Rhodium Transient

José G. Andino and Kenneth G. Caulton*

Department of Chemistry, Indiana University, Bloomington, Indiana 47405, United States

Supporting Information

ABSTRACT: The mechanism of formation of triplet (PNP)RhO and (PNP)Rh(N_2) (PNP = N($SiMe_2CH_2P^tBu_2$)$_2$) from reaction of two molecules of (PNP)Rh with N_2O has been studied by DFT, evaluating mechanisms which (1) involve free N_2, and (2) which effect N/O bond scission in linearly coordinated (PNP)RhNNO. This work shows the variety of modes of binding N_2O to this reducing, unsaturated metal fragment and also evaluates why a mechanism avoiding free N_2 is preferred. Comparisons are made to isoelectronic CO_2 in its reaction with (PNP)Rh.

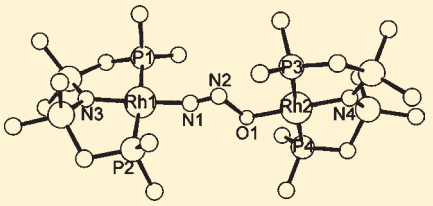

INTRODUCTION

The paucity of success in eliciting reactivity from N_2O toward metal complexes has led to a situation where the number of computational publications rivals the number of experimental results. Because N_2O is an endothermic molecule, synthetic studies have generally sought oxygen atom transfer (eq 1),

$$N_2O \rightarrow N_2 + |\bar{O}| \quad (1)$$

with release of (benign) N_2 as coproduct, and this has indeed been observed.[1] Frustrating the planning of systematic work is the absence of any single experimental structure determination of coordinated N_2O. Since this manuscript was submitted for publication, a structure determination has appeared, and the solution behavior confirms binding, to V(III), to be weak and at the terminal nitrogen.[2] Computational studies have sought to fill that void and concluded that electron transfer *from* metal to N_2O is needed to supplement the very poor Lewis basic character of N_2O for donation *to* a metal.[3−8]

Given that N_2O is a very weakly binding ligand and thus spectroscopic observations on metal N_2O complexes are very rare,[5] density functional theory (DFT) calculations have led the way in our understanding of the interaction of this triatomic species with metal complexes. This triatomic is found to bind only weakly to coordinatively unsaturated metal complexes, and numerous authors have all concluded that the binding is not that of Lewis base donation of N_2O lone pairs to the metal but rather redox character, with metal electrons being donated into the π^* orbitals of N_2O, yielding a net reduction of the triatomic. For example,[9] when N_2O binds (terminal N-bound, and doubly bent) to (PNP)Os(H)$_3$ (PNP = N($SiMe_2CH_2P^tBu_2$)$_2$), the resulting species is (PNP)OsH(H_2)(NNO) where the conversion of two hydrides to coordinated H_2 is an obvious reflection of oxidation of the complex by N_2O. Reduced N_2O species (Scheme 1) are either nitrosoamine, $H_2NN{=}O$, or hydroxyl diimide, $HN{=}N(OH)$, and we calculate that the former is the more stable isomer but by only 3.9 kcal/mol. When doubly deprotonated, N_2O^{2-} (which is isoelectronic with nitrite ion, ONO^-) has two resonance alternatives, which are clearly related to the doubly protonated isomers (Scheme 1). The final generalization from previous computational work is that the thermodynamically favored binding site for metals is at the terminal N (which is still compatible with two resonance alternatives, Scheme 1, for this coordinated ligand), and that the O-bound form is less favored, despite the fact that it may appear mechanistically attractive for reactions leading to metal oxo products. The N-bound form is especially important in that it involves build-up of negative charge on the pendant oxygen (good for attack by a *second* unsaturated metal complex) and is thus on the path toward the oxo transfer for which N_2O is generally employed:

Scheme 1

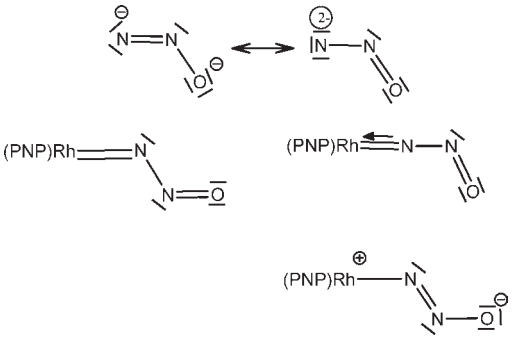

$$N_2O + 2e \rightarrow N_2O^{2-} \rightarrow N_2 + O^{2-}$$

Faced with this background, our previous finding[10] that N_2O effects oxygen atom transfer to rhodium (eq 2) to make the

Received: March 17, 2011
Published: June 22, 2011

unusual species (PNP)RhO stimulated interest in the mechanism of this facile (−30 °C), high yield reaction.

$$2(\mathrm{PNP})\mathrm{Rh} + \mathrm{N_2O} \rightarrow \underset{S=1}{(\mathrm{PNP})\mathrm{RhO}} + \underset{S=0}{(\mathrm{PNP})\mathrm{Rh}(\mathrm{N_2})} \qquad (2)$$

We report here such a DFT computational study of the reaction mechanism, because no intermediates are observed when the reaction is monitored at low temperature. More generally, we are interested in mechanistic features of this reaction which help guide future utilization of N_2O as an oxygen atom transfer reagent.[11,12]

BACKGROUND

The synthesis of (PNP)RhO from N_2O is unusual in that it originates[13] from what is apparently a trivalent rhodium species, thus not an obvious target for the two-electron redox reaction (eq 1) of oxygen atom transfer. Additionally, the species (PNP*)RhH is a particularly unattractive target for coordination of N_2O because the open coordination site is trans to a highly labilizing (trans effect) sp^3 carbon. We already know that (PNP*)RhH reacts with an electronically diverse range of ligands L (CO, CO_2, H_2O, N_2,

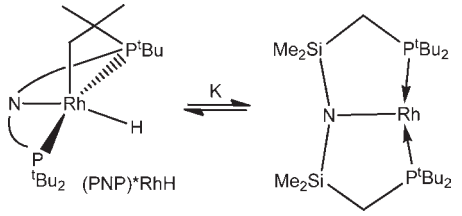

PMe_3) by rapid (time of mixing) C/H reductive elimination, to always form (PNP)Rh^I(L). Because we also know that (PNP*)RhH is in rapid ($\sim 10^3$ s^{-1}) equilibrium and is nearly (2.7 kcal/mol) degenerate with the three-coordinate isomer (PNP)Rh, we will analyze here the mechanism of N_2O reaction beginning with this lower coordinate, monovalent species *in its singlet state*. This is additionally reasonable because the hydride (PNP*)RhH is an unlikely candidate for N_2O binding because the trivalent metal is less reducing than the monovalent metal. Furthermore, because the rhodium reagent is established independently to react fast with N_2 to form the observed coproduct, (PNP)Rh(N_2), a relevant mechanistic question arises: does the actual mechanism of eq 2 involve *free* N_2, or does N_2 formation (N/O bond scission) occur with some Rh/N bond *already established*? Answering this question is one important goal, and it will divide possible mechanisms into two general classes. Thus, we deal here with the question of whether the N_2 is captured by rhodium concurrent with the N/O bond scission, or whether it is first formed as free N_2 and then coordinates to available (PNP)Rh.[10] Relevant here is that a mechanism involving free N_2 might be expected to lead to less than equimolar (PNP)Rh(N_2) product, because, for the first 50% of the reaction, there is more N_2O to trap rhodium reagent than there is N_2.

RESULTS

Geometry optimization (B3LYP functional) of the reactant, singlet (PNP)Rh, yielded the structure in Figure 1. The frontier orbitals of this species (Figure 1) show a LUMO perfectly suited for accepting a reagent lone pair, and a HOMO-1 suited for back bonding to the π^* orbital of the arriving N_2O; such back-donation is of course another name for redox transfer of electrons from metal to N_2O discussed here in the Introduction. Note that the LUMO of N_2O (Figure 2) is completely π^* in character (but relatively high in energy), and any occupancy of this orbital will weaken both the N/N and N/O bonds. The HOMO of triatomic N_2O is primarily a lone pair on terminal N and O, and thus the best overlap for $ON_2 \rightarrow$ Rh bonding would favor a structure bent at the terminal N.

1:1 Adducts. In what follows, to make the problem more computationally tractable as we move to the larger two-rhodium species, we have used a model with PMe_2 groups in place of P^{t}Bu$_2$ groups. We have shown, by comparative calculations of these two models for (PNP)Rh(N_2O) isomeric structures, as well as the overall thermodynamics for eq 2, that energies are not materially altered by this simplification (see Supporting Information).

While the N-bound structure (Scheme 2 and Figure 3) is the most stable adduct (PNP)Rh(N_2O), it has an entirely linear RhNNO unit, indicative of minimal reduction of the N_2O (i.e., the bending shown in Scheme 1). Beginning energy minimization from RhNNO structures bent at one or at both nitrogens returns the above all-linear geometry, meaning that there are no such bent structural isomers. The linearity suggests that it is not forward donation from N_2O to Rh but rather back-donation that dominates the geometry (i.e., best orbital overlap) and hence also dominates the interaction. This is consistent with the ideas discussed above that the strongest binding of N_2O to a metal requires electron transfer.

For (PNP)Rh, HOMO-1, with dπ symmetry, is only 0.12 eV lower than HOMO, which is clearly dz^2. While the LUMO of (PNP)Rh has the correct symmetry for a σ interaction with N_2O, the resulting bent geometry (best $HOMO_{N2O} \rightarrow LUMO_{Rh}$ overlap) would limit the preferred π interaction ($HOMO\text{-}1_{Rh} \rightarrow LUMO_{N2O}$ back-donation) necessary for the subsequent oxidation of monovalent Rh to trivalent.

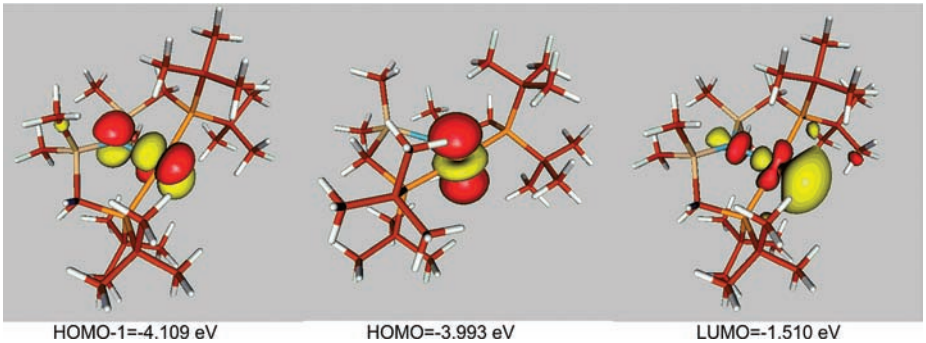

Figure 1. DFT -optimized geometry and frontier orbitals of (PNP)Rh.

dx.doi.org/10.1021/ja202439g |*J. Am. Chem. Soc.* 2011, 133, 12576–12583

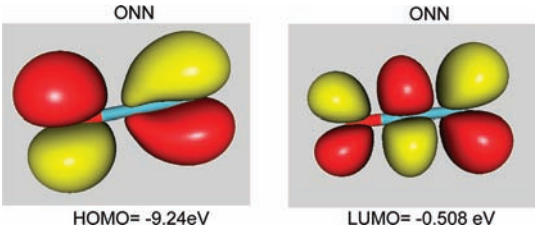

Figure 2. Frontier orbitals of N_2O.

Scheme 2

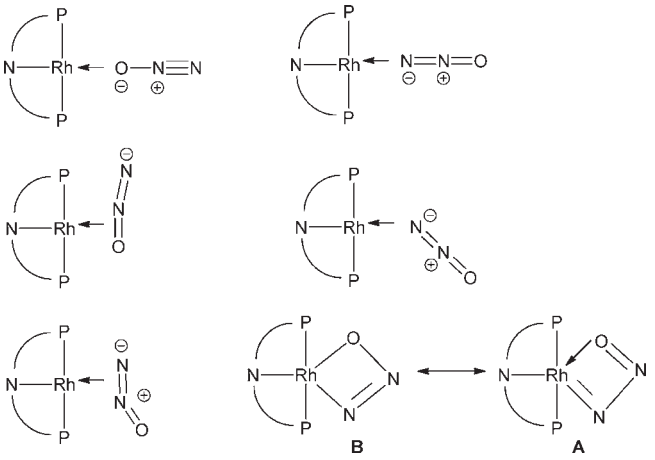

We also considered the possibility that the O-atom transfer reaction (eq 2) could effect spin change by formation of triplet (PNP)Rh(N_2O). We considered triplet adducts with the structure most favored for the singlet that are bound only by one terminal nitrogen of N_2O. In trying to optimize the geometry of a triplet state for adduct (PNP)Rh(NNO), we found the optimization destroyed the Rh/N link by increasing the distance to linear N_2O. Triplet (PNP)Rh does not bind N_2O from this starting geometry.

We considered various other singlet structures with η^1 and η^2-1,2 binding of N_2O to the (PNP)Rh fragment (Scheme 2). We find that an O-bound species (Figure 3) is the least stable structure (by 18.1 kcal/mol), in a species where the Rh/O distance is long (2.16 Å) and the N_2O fragment remains linear and shows no significant modifications of bond lengths from those of free N_2O. Thus, for energetic reasons, this species would only reach a negligible population in any pre-equilibrium and is thus not an attractive mechanistic participant. In brief, the O end of N_2O is apparently not suited for two-electron transfer *from* the metal. This is perhaps due to the smaller oxygen character in the LUMO of N_2O (Figure 2). Lying only 3.5 kcal/mol above linear (PNP)RhNNO is a structure **3** (Figure 3) that binds η^2 through the two nitrogens. For comparison, this structure is the ground state for the isoelectronic (PNP)Rh(CO_2). This η^2-N,N structure has the N/N bond lengthened from free N_2O by 0.07 Å, the N/O bond lengthened by 0.04 Å, and the NNO angle bent to 146°. However, because it does not initiate any Rh/O bond formation, it is not on the direct path to (PNP)RhO and free N_2. A structure-bound η^2 through the NO bond (**5**, Figure 3) is higher in energy by 11.6 kcal/mol. Given errors in the DFT method, we do not consider the energy difference between **2** and **3** to indicate a strongly expressed stability difference.

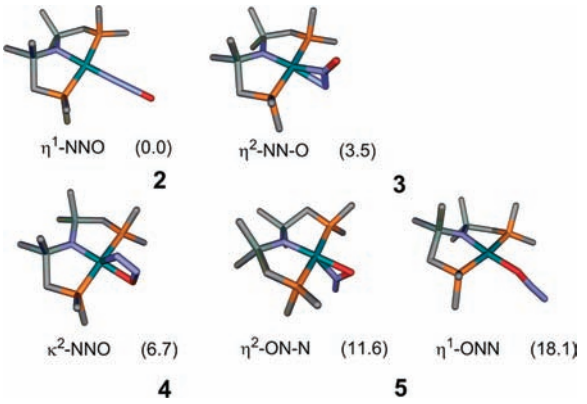

Figure 3. Structures and relative energies (kcal/mol, from DFT) for isomeric (PNP)RhNNO species. Oxygen is shown in red.

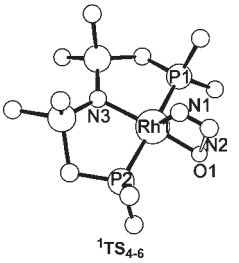

Figure 4. ^{1}**TS**$_{46}$ for conversion of (PNP)Rh(κ^2-N,O-NNO) to (PNP)RhO, ^{1}**6**, and N_2.

When the reaction energy is corrected by $T\Delta S$ at the temperatures employed experimentally, N_2O binding to (PNP)Rh in the most stable structure is calculated to be essentially thermoneutral, consistent with the fact that we do not observe a 1:1 N_2O adduct by NMR at −60 °C.

Mechanism Involving Free N_2. A κ^2-1,3 connectivity (Scheme 2) is of special interest because it is attractive for a [2 + 2] mechanism for forming Rh═O and N≡N units. The fully cyclized structure (**4**, Figure 3) is remarkably close (+6.7 kcal/mol) in energy to linear (PNP)RhNNO; it involves κ^2-N,O binding of a strongly (108.9°) bent N_2O, with a Rh/N distance of 2.00 Å, suggesting this is a Rh^{III} species with an *N*-nitroso imide ligand (**A**, Scheme 2), hence involving Rh═N bonding. However, the bond distances within the ring suggest some participation by the second resonance form **B**, Scheme 2, which is on the path toward complete N/O bond scission. This singlet species is obviously a very attractive candidate for forming the observed rhodium oxo product so we sought a transition state (TS) for N/O bond scission beginning from **4**.

The ^{1}**TS**$_{46}$ for loss of N_2 from the cyclic **4** (Figure 4) was found 18.6 kcal/mol above the cyclic minimum, a barrier too large (even if modified by <10 kcal/mol for $T\Delta S^{\ddagger}$) to agree with the experimental half-life for (PNP)RhO formation at −30 °C. It involves a large (0.7 Å) stretching of the N/O bond and a 0.09 Å shortening of the N/N bond but a much smaller (0.06 Å) lengthening of the Rh/N bond, hence an asynchronous TS with structure late in N/O bond rupture but early in Rh/N scission. Despite this feature, it is not found to proceed to an intact (PNP)Rh(N_2)(O) structure but rather smoothly forms free N_2 and singlet (PNP)RhO, ^{1}**6**. This is consistent with experimental evidence showing no Lewis base (e.g., RCN) binding by (PNP)RhO. Why is the energy of this TS so high?

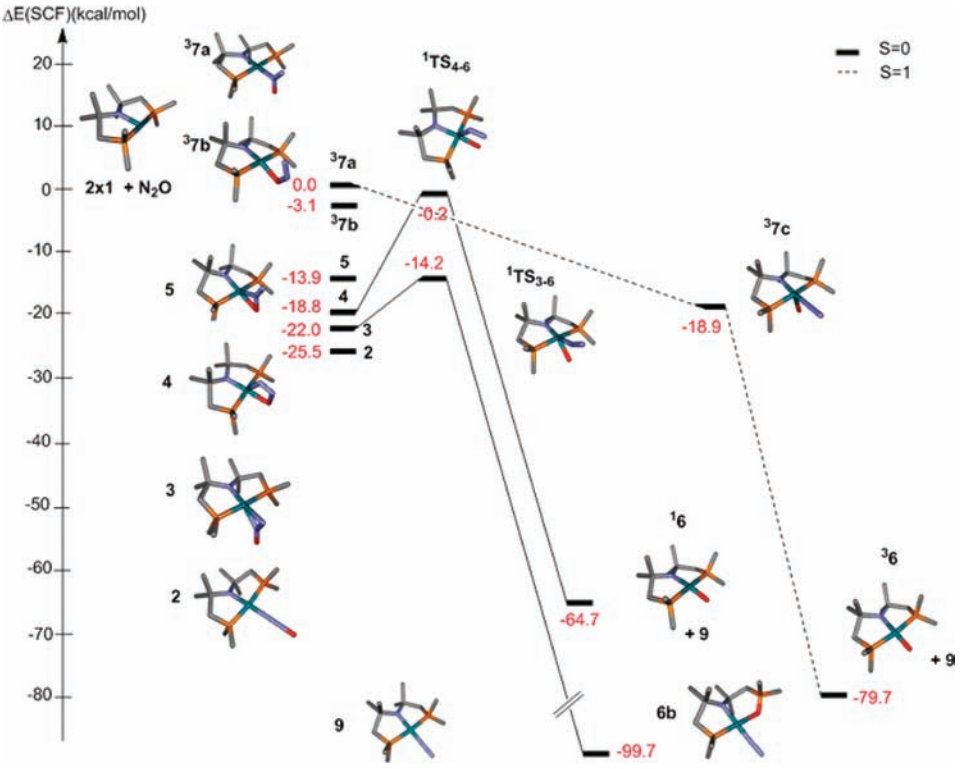

Figure 5. DFT structures and electronic energies (kcal/mol) for conversion of monometallic species to products. All final products shown include capture of liberated N_2 by the second molecule of **1**, to give (PNP)Rh(N_2), **9**.

We suggest that this is because the asynchronous nature of the RhN and NO bond rupture process yields a structure with a highly bent RhNN angle, which clearly lacks the stabilizing (linear) character of all dinitrogen complexes; in brief, it requires mainly bond breaking and provides little compensatory bond making.

We also located ^{1}**TS$_{36}$**, which connects (Figure 5) not to (PNP)-RhO but instead to **6b**, where the oxo ligand has oxidized one PNP phosphorus, with N_2 remaining bound to rhodium; this shows that phosphine oxidation is an ever-present threat but it is not observed experimentally, and this process was considered unrealistic.

We next consider the N/O scission event as a possible spin crossing point. Triplet (PNP)Rh(NNO), initially bound as either η^2-NN or η^2-NO, both optimize (Figure 5) to a geometry ^{3}**7a** where the N_2O ligand is bound primarily via its internal nitrogen (the Rh/O separation is 2.65 Å). This is an excited state,

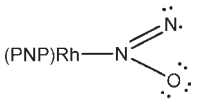

^{3}**7a**

lying 25.5 kcal/mol higher than the singlet structure **2**. This high energy confirms the generality that triplet states have unattractive high energies for (PNP)RhL species. Why does the triplet sacrifice one metal/ligand atom contact? The spin densities show that this is well described as the result of a M → LCT excitation, because the spin density at Rh is only 0.86 e, with the majority of the remainder at N1 (the dissociated nitrogen, at 0.73 e) and 0.19 e each at O1 and at amide N3. This is thus adequately idealized to Lewis structure ^{3}**7a**, which shows net one-electron reduction of the N_2O to its radical anion, and thus the species is best described at (PNP)Rh^{II}($N_2O^{-\bullet}$). The resulting η^1 ligand binding thus resembles that of N-bound (PNP)Rh^{II}(NO_2), because NO_2^- and $N_2O^{-\bullet}$ differ by only one electron. Because this triplet has no Rh/O bond, it appears irrelevant to the formation of (PNP)RhO and N_2.

Figure 5 shows some aspects of the PES for single-rhodium approaches to the formation of (PNP)RhO. We expect a low barrier for initial capture of N_2O by (PNP)Rh at any collision geometry, hence easy access to **2**−**5**; this same ready adduct formation was found in calculations for Cp_2Ti reacting with N_2O_4. Because **2** and **3** contain no Rh/O bond, they do not continue directly toward product in a single-rhodium pathway.

Species ^{3}**7b** is an isomer of ^{3}**7a** where it is oxygen rather than the central nitrogen that binds to the metal. Like ^{3}**7a**, it has spin density 0.92e at Rh, and spin 0.90e on the moiety N_2O, indicating that it is again divalent rhodium and radical anion N_2O^{1-}, now coordinated via oxygen. The N/O bond is long (1.37 Å). Bond angles at oxygen (108.7°) and at N1 (125.4°) suggest sp^3 and sp^2 hybridization, respectively, all consistent with Lewis structure ^{3}**7b**. The Rh/N3 distance, 2.93 Å, is not bonding. ^{3}**7b** connects to ^{3}**7c**, which is a square pyramidal oxo dinitrogen complex in a triplet state with oxo trans to the empty site but a long (2.135 Å) Rh/O distance. It is highly exothermic for ^{3}**7c** to lose N_2 to form the triplet oxo product ^{3}**6**. Spin densities in ^{3}**7c** are at O (1.28e) and Rh (0.70e).

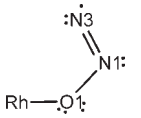

^{3}**7b**

The energy for binding N_2 to (PNP)Rh is −32.8 kcal/mol, which has been incorporated into Figure 5. Experimentally, this reaction is fast and goes to completion.[13]

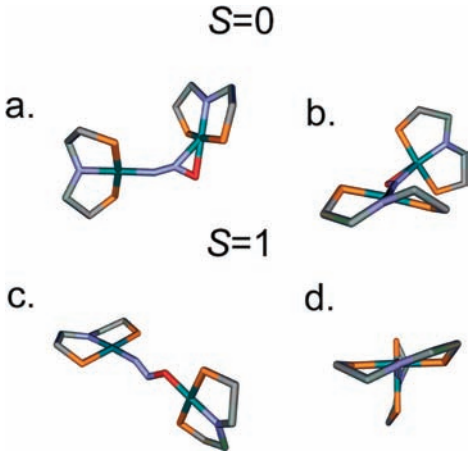

Figure 6. Skeletal structures for singlet (^{1}**8**, a and b) and triplet (^{3}**8**, c and d) (PNP)RhNNORh(PNP) species; triplet is more stable by 7.2 kcal/mol. Illustrations b and d are viewed down one (pincer N)−Rh bond of the P_2N_2-coordinated rhodium, to show the orientation of the second, more distant (PNP)Rh moiety.

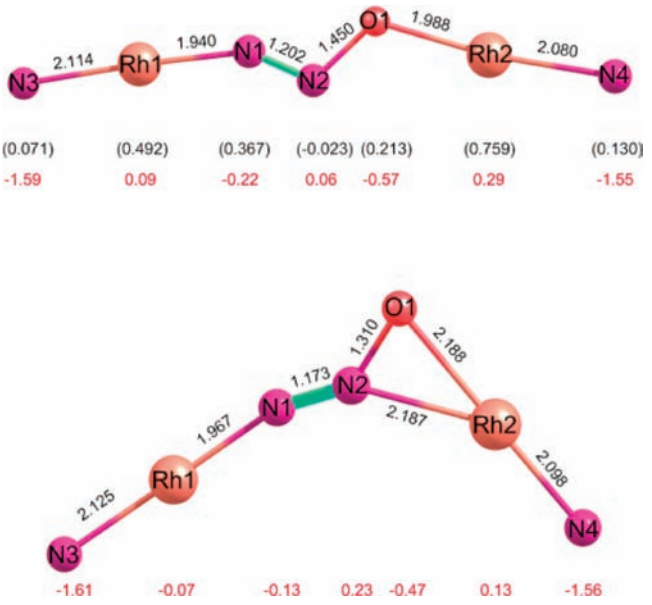

Figure 7. Bond lengths (Å, black), NPA charges (red), and spin densities (in parentheses) in singlet (^{1}**8**, lower) and triplet (^{3}**8**, upper) (PNP)RhNNORh(PNP).

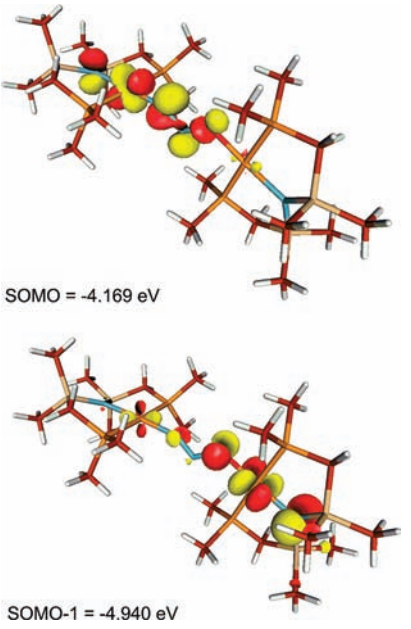

Figure 8. Isodensity diagrams of two SOMO's of triplet (PNP)-RhNNORh(PNP), ^{3}**8**, viewed in the same orientation as in Figure 6c.

Mechanism Avoiding Free N_2. We now bring a second (PNP)Rh unit into consideration. Note that, from the moment any RhNNORh unit is formed, the central problem is the flow of electrons, potentially from *two* metal centers, in the redox process (finally making Rh(III) from Rh(I) in the process of $N_2O + 2e^- \rightarrow N_2 + O^{2-}$), complicated by the need to decide the optimum structure at which to change from singlet to triplet surfaces.

Considering species (PNP)Rh(NNO)Rh(PNP) immediately raises the question of whether such species has an electron distribution closer to Rh^{III} and Rh^{I} or instead more like two Rh^{II}; the latter immediately provides the opportunity to have the two d^7 species couple antiferromagnetically (hence a singlet spin state) or ferromagnetically (hence a triplet). This point is of special importance because it could provide the spin crossing needed to directly form (PNP)RhO in its observed triplet ground state. Certainly the geometry of singlet and triplet (PNP)Rh^{II}(NNO)Rh^{II}(PNP) would be anticipated to be very similar, because the spins in the triplet are expected to be so distant from each other, and a structural match can facilitate spin crossing. Among mechanisms which recruit a second (PNP)Rh fragment to attack some (PNP)Rh(N_2O) species, we discount all but the η^1-bound PNPRhN_2O species (Figure 3) on the grounds of extreme steric improbability of others. All of our previous experimental studies with the tetra-tBu-substituted pincer show the absence of closely (i.e., one- or two-atom-) bridged dimetal species. We therefore proceeded with "extended" (PNP)Rh(N_2O) structures, to seek species where the N_2O bridges two metals in a minimally congested form; we considered both singlet and triplet species of composition (PNP)RhNNORh(PNP).

a. Dimetal Intermediates. We located two minima (Figure 6), one, ^{3}**8**, a triplet with one Rh bonded to one terminal N and the other Rh bonded to O. This is strongly bent at all three N_2O atoms; an unreduced N_2O moiety would be expected to be linear at the central nitrogen atom. Beginning singlet optimizations from this triplet (PNP)RhNNORh(PNP) structure, we also located (Figure 6) a singlet, ^{1}**8**, which, curiously, has the NO substructure η^2 bonded to one Rh. In both, the N2−O1 distance is long, 1.31−1.45 Å, and the Rh1−N1 distance is short (1.97−1.94 Å, both vs 1.209 and 1.985 Å in (PNP)Rh(η^1-NNO)).

The spin densities in the triplet (Figure 7) show higher spin population at the fragment which is becoming (PNP)RhO with less on the second rhodium (0.49e) and its attached N_2O nitrogen (0.37e).

Note also that the pincer amide *nitrogen* at the oxo end has spin density, with less at the pincer N of the other, more reduced metal end. The two SOMOs in the unrestricted calculation for the triplet (Figure 8) show a logical segregation of electrons onto separate metal centers, and also some onto the pincer nitrogen, with of course some contribution from the bridging NNO substructure.

dx.doi.org/10.1021/ja202439g |*J. Am. Chem. Soc.* 2011, 133, 12576–12583

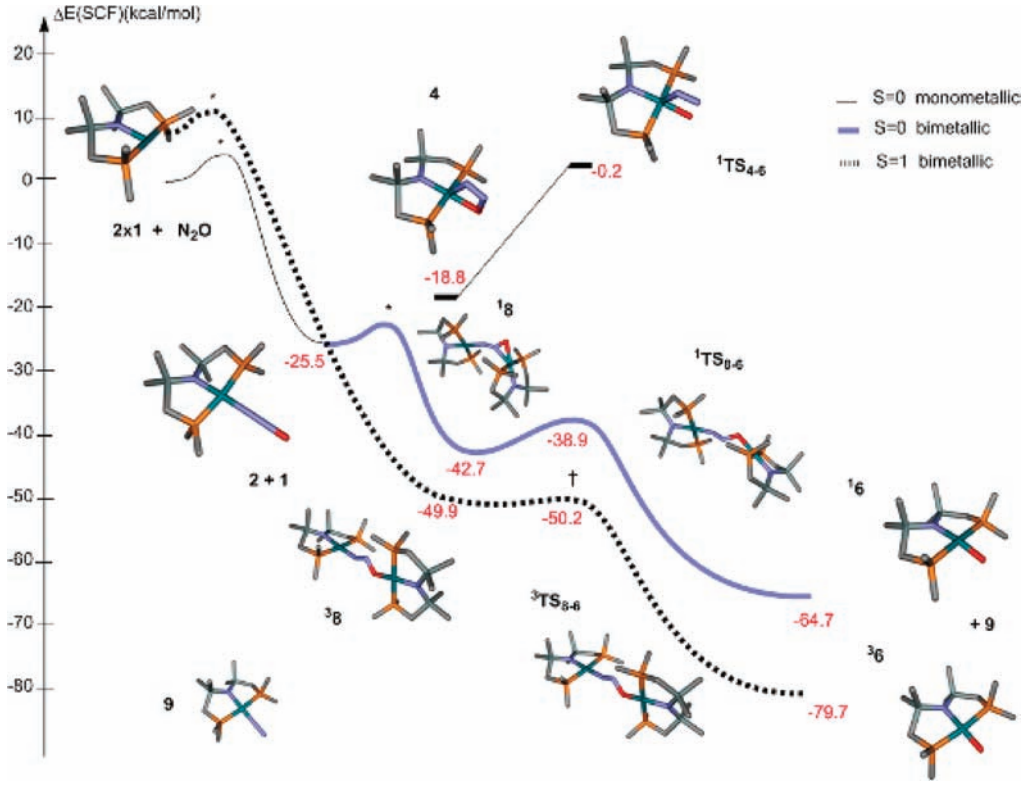

Figure 9. PES for alternative mechanisms for the bimetal mechanism, involving both singlet and triplet states. An asterisk (*) indicates species not located. For comparison, the lowest energy of N/O bond scission at a single metal center is repeated here from Figure 5. A dagger symbol (†) indicates the minimum and TS found at energies whose difference is within error limits of the DFT method.

This segregation is stabilizing by separating these electrons and thus minimizing their accompanying repulsion. Such segregation is possible because the two RhP_2N planes are nearly orthogonal in the triplet (Figure 6), so that orthogonal π systems of the bent NNO substructure are accessed. Consistent with this logic, the triplet is found to be 7.2 kcal/mol below the energy of the singlet. Note also that the Rh/O bond is shorter, and the N/N and the NO bonds are longer in the triplet vs the singlet, showing greater progress toward product on the triplet path. Consistent with this, NPA atomic charges (Figure 7) for these two species show the N_2O substrate to be 0.36 e more reduced (negative) in the triplet; of this difference, 89% (0.32 e) comes from the two metals. As shown in Figure 9, we suggest that the spin crossing occurs at or just prior to forming the two (PNP)RhNNORh(PNP) spin isomers **8**.

b. TS for N/O Scission from Dimetal Intermediates. We also located a ^{3}**TS$_{86}$** for the triplet species cleaving its N/O bond, thus a TS for formation of the observed products triplet (PNP)RhO, ^{3}**6**, and singlet (PNP)Rh(N_2), **9**. This lies so close to triplet (PNP)RhN_2ORh(PNP), ^{3}**8**, that this is essentially a barrierless N/O bond scission. ^{3}**TS$_{86}$** is, structurally, very early because it is a very exothermic process to form products (Hammond Postulate). The triplet ^{3}**TS$_{86}$** shows its major structural alteration from ^{3}**8** being lengthening (+0.10 Å) of N2/O1, shortening (by 0.02 Å) of N2/N1, and a 10° increase in angle Rh1/N1/N2 (i.e., progress toward a linear RhN_2 complex). Forming the observed products requires reducing one metal to monovalent state, forming (PNP)Rh(N_2), **9**, so this means that the (PNP)RhO fragment, as it is assembled, must suffer oxidation from what it was in ^{3}**8**. The primary spin density change from ^{3}**8** to its ^{3}**TS$_{86}$** is a 50% increase at oxygen; corresponding NPA atomic charge *changes* are all less than 0.03. Given the distributed character of spin in the SOMOs (Figure 8), most of the spin flow will occur following ^{3}**TS$_{86}$**.

The curious feature of η^2 bonding of the NO substructure in the singlet (PNP)RhNNORh(PNP) species ^{1}**8** vs η^1-NNO bonding in (PNP)RhN_2O, **2**, would appear to be a nonleast motion aspect which could lead to higher energy for transforming this into the final products, and indeed there *is* a barrier (Figure 9) to form that ^{1}**TS$_{86}$**. The main change from singlet (PNP)RhNNORh(PNP) to ^{1}**TS$_{86}$** is to lose the Rh2N2 interaction; angle Rh2O1N2 increases by 43°, and N1N2O1 decreases by 12°, the latter apparently reflecting rehybridization as the N2O1 bond breaks. Noteworthy is the modest lengthening of N2/O1 (+0.04 Å). From ^{1}**8** to ^{1}**TS$_{86}$**, NPA charges become more positive at both metals (oxidation), and more negative at oxygen, but also at both N_2O nitrogens (see Supporting Information). The overall PES for the competing mechanisms is shown in Figure 9 and favors the mechanism avoiding free N_2.

DISCUSSION

It is useful to recognize that N_2O is isoelectronic with CO_2, whose adduct, (PNP)Rh(CO_2), is already established to be bound η^2-C,O. This establishes a key difference between CO_2 and N_2O products, which must be attributed to the lack of symmetry of the latter triatomic and thus the electrophilicity of the carbon which is not well developed at the central atom in N_2O; to see this, note (Figure 2) the central N participation in the HOMO of N_2O, while carbon is absent by symmetry in CO_2. To continue this N_2O/CO_2 comparison, the calculated reaction energy for eq 3 is only −1.2 kcal/mol. This difference originates in the inherently endothermic character of N_2O (contrast CO_2),

dx.doi.org/10.1021/ja202439g |J. Am. Chem. Soc. 2011, 133, 12576–12583

but the reaction of eq 3 (not observed experimentally) is probably additionally prevented by the steric congestion in the approach of (PNP)Rh to η^2-CO_2.

$$(PNP)Rh(\eta^2\text{-}CO_2) + (PNP)Rh \rightarrow (PNP)Rh(CO) + (PNP)RhO\ (S = 1) \quad (3)$$

The faster mechanism for eq 2 involves binding first one and then a second (PNP)Rh fragment to N_2O. In general, when a conjugated σ-donor ligand bonds to one metal, ligand nucleophilicity is reduced and thus its binding energy to a second metal is also reduced. The fact that, in this N_2O study, the energy of the second binding event (−24.4 kcal/mol) is nearly as favorable as the first (−25.5 kcal/mol), a kind of "cooperativity", shows that the first metal makes the N_2O more electron rich and more nucleophilic and is thus another indication that this first binding event reduces N_2O. In general, binding of N_2O here is much more favorable than in other cases[1] because of the high reactivity (unsaturation and reducing power) of the (PNP)Rh fragment.

We anticipated that, if the spins in a triplet were separated on the two different metals, then it was likely that the geometry of a species (PNP)RhN_2ORh(PNP) would be very similar in singlet and triplet states; if these spin states were nearly degenerate, this then would suggest that this species is where the spin crossing between spin states would occur. In fact, our calculations showed the limits of this structural expectation: the coordination number of the Rh becoming a triplet oxo species is lower, apparently in response to a half-filled orbital not being Lewis acidic toward the internal N of N_2O (Figure 7). However, the somewhat unusual rhodium oxidation state +2, especially in the presence of an amide ligand (PNP) to delocalize spin, participates in certain of the species we have evaluated computationally. For example, the bending of the NNO moiety in ^{3}**8**, as well as the NN and NO distances there, makes it resemble doubly deprotonated HN═N−OH, hence a coordinated, bridging N_2O^{2-} ion; the overall spin state then suggests divalent rhodium attached to either end. The redox process has, at this stage, been accomplished by one-electron transfer from each Rh(I) reagent.

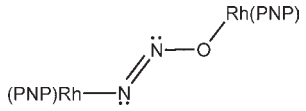

It is of interest that the calculated reaction energy for the eq 4 is −7.3 kcal/mol. Oxidation of N_2 to N_2O makes it a worse ligand. Thus, although this confirms expectation that N_2 is a better ligand than N_2O (in its most stable structure), the small difference between these two is surprising.

$$(PNP)Rh(NNO) + N_2 \rightarrow (PNP)Rh(N_2) + N_2O \quad (4)$$

The case of two Cp_2Ti reacting with N_2O to ultimately form $[Cp_2Ti]O[TiCp_2]$ and free N_2 has some significant differences from the rhodium case at hand. As for rhodium, each titanium is a two-electron reducing agent,[4] but the final product contains *equivalent* metals, hence both Ti^{III}; for eq 1, two electrons come from one rhodium, so the two metals are *inequivalent* in the *products*. For the Ti^{II} case, DFT analysis indicates that the fastest path to product involves single-electron reduction of N_2O, forming $Cp_2Ti(NNO)$, and then a second single-electron reduction of this adduct via attack at oxygen by additional Cp_2Ti and collapse of the resulting $[Cp_2Ti]NNO[TiCp_2]$ to $[Cp_2Ti]_2O$ and free N_2; thus, Cp_2TiO and $Cp_2Ti(N_2)$, the analogues of what we find in our rhodium system, are not thermodynamically viable products, so a bridging oxo is formed. The μ-oxo species is formed by an intramolecular rearrangement of the species $[Cp_2Ti]NNO[TiCp_2]$. In the contrasting case of $(R_3SiO)_3WCl$, the partitioning of products and reducing power is more like that seen for (PNP)Rh: the products are $(R_3SiO)_3WCl(O)$ and $(R_3SiO)_3WCl(N_2)$.[14−16]

In summary, one (PNP)Rh center is not a strong enough reducing agent to abstract O from N_2O; two such units are required to do this, and these also find a kinetically facile mechanism for doing so. For comparison, because the reaction of (PNP)Rh and CO_2 stops at (PNP)Rh(η^2-CO_2), this carbon oxide cannot even be deoxygenated (to form (PNP)RhO and (PNP)Rh(CO)) because of a greater stability than N_2O (evident because the reaction of N_2O with CO to form N_2 and CO_2 is highly exothermic).

Why, in most general terms, is the mechanism here, which avoids free N_2, faster? We suggest that it is because "early" use of the second (PNP)Rh unit better permits bond formation to accompany bond cleavage, so that there is some concerted compensation for N/O bond stretching. The mechanism involving free N_2 only recovers the stabilization (−32.8 kcal/mol) of bonding N_2 to (PNP)Rh late in the mechanism and thus involves a earlier high energy mechanistic step. In general, for reactions with stoichiometry "2 M + substrate", this is a principle to consider for the most efficient mechanism. The Cp_2Ti example discussed above shows that the same is true even if coordination of N_2 is not favored in the product; the generality of this mechanistic principle is clear.

■ ASSOCIATED CONTENT

Supporting Information. Full details of computational study. This material is available free of charge via the Internet at http://pubs.acs.org.

■ AUTHOR INFORMATION

Corresponding Author
caulton@indiana.edu

■ ACKNOWLEDGMENT

This work was supported by the National Science Foundation, CHE-0749386.

■ REFERENCES

(1) Tolman, W. B. *Angew. Chem., Int. Ed.* **2010**, *49*, 1018.
(2) Piro, N. A.; Lichterman, M. F.; Harman, W. H.; Chang, C. J. *J. Am. Chem. Soc.* **2011**, *133*, 2108.
(3) Fan, H.; Caulton, K. G. *Polyhedron* **2007**, *26*, 4731.
(4) Yu, H.; Jia, G.; Lin, Z. *Organometallics* **2009**, *28*, 1158.
(5) Paulat, F.; Kuschel, T.; Nather, C.; Praneeth, V. K. K.; Sander, O.; Lehnert, N. *Inorg. Chem.* **2004**, *43*, 6979.
(6) Incremental reduction by multipoint binding to three weakly reducing (Cu^I) centers has been described. See Gorelsky, S. I.; Ghosh, S.; Solomon, E. I. *J. Am. Chem. Soc.* **2006**, *128*, 278.
(7) Khoroshun, D. V.; Musaev, D. G.; Morokuma, K. *Organometallics* **1999**, *18*, 5653.
(8) Harman, W. H.; Chang, C. J. *J. Am. Chem. Soc.* **2007**, *129*, 15128.
(9) Lee, J.-H.; Pink, M.; Tomaszewski, J.; Fan, H.; Caulton, K. G. *J. Am. Chem. Soc.* **2007**, *129*, 8706.

(10) Verat, A. Y.; Fan, H.; Pink, M.; Chen, Y. S.; Caulton, K. G. *Chem.—Eur. J.* **2008**, *14*, 7680.
(11) Harrold, N. D.; Waterman, R.; Hillhouse, G. L.; Cundari, T. R. *J. Am. Chem. Soc.* **2009**, *131*, 12872.
(12) Vaughan, G. A.; Rupert, P. B.; Hillhouse, G. L. *J. Am. Chem. Soc.* **1987**, *109*, 5538.
(13) Verat, A. Y.; Pink, M.; Fan, H.; Tomaszewski, J.; Caulton, K. G. *Organometallics* **2008**, *27*, 166.
(14) Kuiper, D. S.; Wolczanski, P. T.; Lobkovsky, E. B.; Cundari, T. R. *J. Am. Chem. Soc.* **2008**, *130*, 12931.
(15) Kuiper, D. S.; Douthwaite, R. E.; Mayol, A.-R.; Wolczanski, P. T.; Lobkovsky, E. B.; Cundari, T. R.; Lam, O. P.; Meyer, K. *Inorg. Chem.* **2008**, *47*, 7139.
(16) Veige, A. S.; Slaughter, L. M.; Lobkovsky, E. B.; Wolczanski, P. T.; Matsunaga, N.; Decker, S. A.; Cundari, T. R. *Inorg. Chem.* **2003**, *42*, 6204.